International Journal of Automation and Computing 9(3), June 2012, 325-330
DOI: 10.1007/s11633-012-0651-3

Purcell's Swimmer Revisited

M. Siva Kumar[1] P. Philominathan[2]

[1]Faculty, Oman Dental College, P.O. Box 835, Postal Code 116, Sultanate of Oman

[2]Research and PG Department of Physics, AVVM Sri Pushpam College, Poondi 631503, India

Abstract: Purcell's swimmer was proposed by E. M. Purcell to explain bacterial swimming motions. It has been proved experimentally that a swimmer of this kind is possible under inertial-less and high viscous environment. But we could not investigate all the aspects of this mechanism through experiments due to practical difficulties. The computational fluid dynamics (CFD) provides complementary methods to experimental fluid dynamics. In particular, these methods offer the means of testing theoretical advances for conditions unavailable experimentally. Using such methodology, we have investigated the fluid dynamics of force production associated with the Purcell's swimmer. By employing dynamic mesh and user-defined functions, we have computed the transient flow around the swimmer for various stroke angles. Our simulations capture the bidirectional swimming property successfully and are in agreement with existing theoretical and experimental results. To our knowledge, this is the first CFD study which shows the fact that swimming direction depends on stroke angle. We also prove that for small flapping frequencies, swimming direction can also be altered by changing frequency-showing breakdown of Stokes law with inertia.

Keywords: Very low Reynolds number flow, swimming motion of bacteria, dynamic mesh, Purcell's swimmer, Stokes flow.

1 Introduction

The swimming mechanism of microscopic organisms is unique and fundamentally different from swimming of other large animals. Such self-propulsion comes under very low Reynolds number hydrodynamics where the motion is dominated by viscous forces. Due to small sized bodies, inertial forces are negligible and any swimming mechanism involving reciprocal motion will result in zero net displacement[1].

One of the very first models explaining the very low Reynolds number swimming motion was from Purcell[2]. He proposed a hypothetical construct called three-linked swimmer capable of swimming at very low Reynolds numbers. It is later reported that the Spiroplasma melliferum propels in a very similar way[3]. The three-linked Purcell's swimmer overcomes the reciprocal motion by alternately moving fore and rear links. Such swimmer is capable of swimming in both forward and backward direction. What determines the direction of such a swimmer was puzzling for more than two decades until Becker et al.[4] showed that it is the stroke amplitude of the flapping links that determines swimming direction.

Purcell's swimmer, which was invented as "the simplest animal that can swim that way", is not simple to analyze at all. But still Purcell's swimmer has been studied extensively in recent years using various methods[5−7]. There are difficulties involved in studying about Purcell's swimmer using experiments. Only few experiments are conducted so far to investigate the swimmer's behavior.

The modern computational fluid dynamics (CFD) complements experimental fluid dynamics by providing alternative means of simulating real flows. In particular, these methods offer the means of testing theoretical advances for conditions unavailable experimentally. We have used such CFD simulations to study Purcell's swimmer and captured its important swimming characteristics. By employing dynamic mesh and transient (unsteady) solving approach, we have calculated the pressure distribution, velocity field and hydrodynamic force during the swimming motion. The results obtained are in good agreement with other existing theories on very low-Reynolds number flow. More importantly our simulations capture the bidirectional swimming behavior and prove that, in addition with stroke angle, flapping frequency also determines the swimming direction. As per our knowledge, this is the first complete CFD based study, capable of showing the bidirectional swimming behavior of three-linked swimmer.

The remaining part of this paper is organized as follows. After describing about the Purcell's swimmer in next section, we discuss self-propulsion models and theories related with very low Reynolds number swimming motion. In Section 4, some reported experiments related with Purcell's swimmer are discussed. Section 5 presents the CFD model, including mesh generation and dynamic meshing. The results and findings are presented in Section 6. In Section 7, we have presented conclusions and future work.

2 The three-linked swimmer

The Purcell's swimmer contains a middle link of length b connected to two arms of equal length a, each arm is capable of rotating alternately by an angle $\pm 2\gamma$ relative to the middle link. This swimmer undergoes four different configurations during every cycle of swimming which causes net translation without rotation (see Fig. 1).

3 Self-propulsion models

The inertial parts of Navier-Stokes equations are negligible for very low Reynolds swimming due to dominant viscous forces. Therefore, these equations are simplified to the Stokes equation

$$\Delta.u = 0 \tag{1}$$

$$\mu\Delta^2 u = \Delta p \tag{2}$$

Manuscript received June 24, 2011; revised July 21, 2011

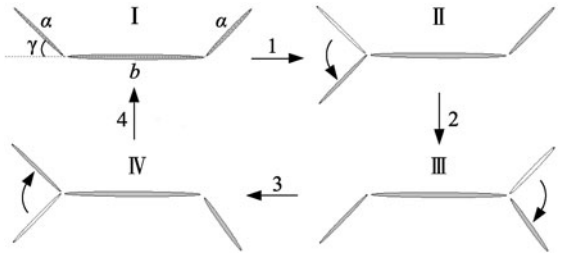

Fig. 1 The Purcell's swimmer with three links and two joints. Changing configurations from I–IV during a cycle indicates non-reciprocal motion – a characteristic feature of very low Reynolds number swimming motion.

where u is the velocity, p is the pressure field, and μ is the dynamic viscosity. Most importantly, the Stokes equations are linear in u. There are two main theories to explain this type of swimming mechanism. They are resistive-force theory and slender-body theory (For a recent review on this topic, see our recent paper [8]).

The resistive-force theory[9] provides relationship between the velocity of the object and the frictional force as $Ru = F$ (R is the resistance matrix and F is the force). More specifically,

$$\int_{\Gamma(s)} \boldsymbol{n}\sigma \mathrm{d}\Gamma = -\left[\frac{2\pi\mu}{\ln(\frac{2}{\varepsilon})}\right](2I - \tau\tau)u(s) + \mathrm{O}[\ln^{-2}(\frac{2}{\varepsilon})] \quad (3)$$

where s is the arc-length along the center-line, Γ is the perimeter of the slender-body cross-section, ε is the slenderness ratio of diameter to length, τ is the tangential vector, and u is the local velocity. The force distribution along the body can be obtained by solving the system of equations with boundary conditions on the surface.

The slender-body theorem replaces the body in terms of fundamental singularities, such as stokeslet or doublet which are solutions of the Stokes equation. The stokeslet represents the velocity distribution induced by a point force applied to the fluid and the doublet represents the limiting velocity field as a source approaches a sink infinitesimally[10].

The velocity and pressure fields caused by a stokeslet and a doublet located at the origin of a Cartesian coordinate system are given by the following equations:

Stokeslet:

$$u = \frac{F}{8\pi\mu}\left(\frac{x^2+l^2}{l^3}, \frac{xy}{l^3}, \frac{xz}{l^3}\right), \; p = \frac{Fx}{4\pi l^3} \quad (4)$$

Doublet:

$$u = \frac{Fr^2}{16\pi\mu}\left(\frac{1}{l^3} - \frac{3x^2}{l^5}, -\frac{3xy}{l^5}, -\frac{3xz}{l^5}\right), \; p = 0 \quad (5)$$

where (x, y, z) are the coordinates of a field point, F is the point force at the origin, l is the distance from the origin to the field point, and r is the radius of the slender-body.

4 Experimental studies

An unpublished work from Bzdega et al.[11] explains the construction of a two-paddled robotic swimmer capable of swimming in granular media. The driving mechanism consisted of two computer-controlled stepper motors mounted on a plate suspended above the surface of the granular medium. The paddles were inside the granular bed consisting of 5 mm diameter glass beads. They have studied the parameters affecting the swimming motion and found similar to Purcell's two-linked swimmer swimming in viscous fluid.

Brian[12] built a three linked swimmer that successfully proved that a swimmer of this kind can swim forward in the Stokes limit. He proved that displacement per cycle vary when the length of the arms were changed. Due to practical difficulty was not any experiment conducted with the variation of stroke angle or flapping frequency.

Owing to the difficulties in measuring hydrodynamic force and controlling various parameters including stroke angles, there were only few experiments conducted so far. No experiment proved the existence of bidirectional swimming behavior of three-linked swimmer. Therefore we have employed CFD simulations to study Purcell's swimmer in detail.

5 Materials and methods

5.1 The CFD model

The incompressible, unsteady Navier-Stokes equations are given by

$$\begin{aligned}
&\frac{\partial u}{\partial t}+u\frac{\partial u}{\partial x}+v\frac{\partial u}{\partial y}+w\frac{\partial u}{\partial z}=-\frac{1}{\rho}\frac{\partial p}{\partial x}+v\left(\frac{\partial^2 u}{\partial x^2}+\frac{\partial^2 u}{\partial y^2}+\frac{\partial^2 u}{\partial z^2}\right)\\
&\frac{\partial v}{\partial t}+u\frac{\partial u}{\partial x}+v\frac{\partial u}{\partial y}+w\frac{\partial u}{\partial z}=-\frac{1}{\rho}\frac{\partial p}{\partial y}+v\left(\frac{\partial^2 v}{\partial x^2}+\frac{\partial^2 v}{\partial y^2}+\frac{\partial^2 v}{\partial z^2}\right)\\
&\frac{\partial w}{\partial t}+u\frac{\partial u}{\partial x}+v\frac{\partial u}{\partial y}+w\frac{\partial u}{\partial z}=-\frac{1}{\rho}\frac{\partial p}{\partial z}+v\left(\frac{\partial^2 w}{\partial x^2}+\frac{\partial^2 w}{\partial y^2}+\frac{\partial^2 w}{\partial z^2}\right) \quad (6)
\end{aligned}$$

with the equation of continuity,

$$\frac{\partial u}{\partial x} + \frac{\partial v}{\partial y} + \frac{\partial w}{\partial z} = 0 \quad (7)$$

where x, y and z are the axes of the orthogonal coordinate system. u, v, and w are the fluid velocity vectors in each direction, respectively. p is the pressure and ρ is the fluid density. Turbulence quantities are not considered as the flow is laminar. Fluid variables are made dimensionless with respect to the uniform inflow u, the length of the arm a, and the fluid density ρ, respectively.

The dimensionless parameter Reynolds number is defined as[13]

$$R_e = \frac{a^2\omega\rho}{\mu} \quad (8)$$

where ω is the rotational speed.

With a value of viscosity $100\,\mathrm{m^2/s}$, density $760\,\mathrm{kg/m^3}$, length 0.006 m, and the rotational speed $1.5\,\mathrm{rad/s}$, the Reynolds number for this study becomes closer to 10^{-3} which is a case of very low Reynolds number flow.

The governing equations are discretized using the finite volume method (FVM) with a first order implicit solver approach. The simulations are carried out for 800 time steps with time step size of 0.005 s. The pressure velocity coupling of the continuity equation is achieved using the

SIMPLE algorithm which is valid for the small time steps used in the simulation.

5.2 Mesh generation and dynamic meshing

The geometry and two-dimensional (2D) mesh as in Fig. 2 (a), was created using Gambit 2.4.6 – an integrated pre-processor for CFD analysis from Ansys Inc. The computational mesh consists of 19 138 cells, 29 377 faces and 10 237 nodes. There were 2 partitions with 2 cell zones and 7 face zones. The walls of the links were modeled as no-slip wall.

Due to motion of the links, the shapes of the boundaries are changing and therefore dynamic mesh model is utilized. User-defined functions (UDF) were used in describing the flapping motion of the swimmer. To dynamically update mesh, spring-smoothing methodology is adopted. The remeshing is done using local remeshing method[14]. Figs. 2 (b)–(d) show the meshing at various time intervals of a cycle.

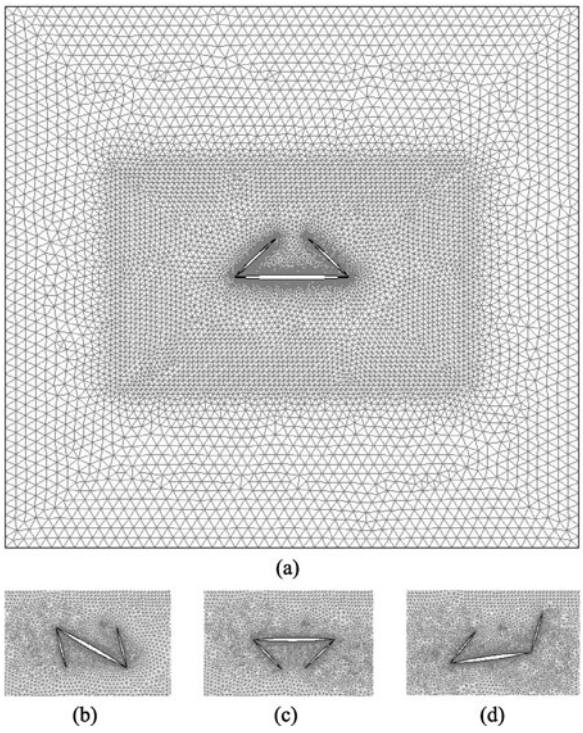

Fig. 2 (a) Three-linked swimmer mesh and geometry for the stroke angle 270 ° and at time $t = 0$. Dynamic mesh updates at times (b) $t = 1$ s, (c) 1.5 s and (d) 3.75 s

The computations were carried out using Ansys® Fluent 13 on a PC with Intel® Core™ Dual 2.16 GHz CPU with 4 GB memory. Separate meshes were created for each stroke angle and simulations were carried out individually for a period of full cycle time. The post-processing of the results is done using CFD-post from Ansys Inc.

6 Results and discussions

6.1 Pressure distribution

The computations were carried out by moving links through user-defined function for the stroke angles of 60 °, 130 °, 200 °, 250 °, 270 ° and 300 °. The pressure distributions for 130° and 250° stroke angles at various time intervals are shown in Figs. 3 and 4. It is seen clearly that in the case of stroke angle 130 ° the horizontal displacement after four cycle time is in the forward direction of the swimmer. In the case of 250 ° stroke angle, the horizontal displacement after four cycle time is in backward direction.

As the dominant forces causing the displacement are viscous forces in very low Reynolds number domain, pressure distribution do not play any significant role. But however, due to non-reciprocal flapping nature there exists asymmetric distribution of pressure contours which indicates horizontal motion.

6.2 Hydrodynamic force

The non-dimensional hydrodynamic force along the horizontal direction of the swimmer is monitored for each stroke angle over a full cycle time. Fig. 4 shows the comparison of forces over various stroke angles. Forward direction (left) of the swimmer is taken as positive and backward as negative. Therefore, time-averaged force is positive for the angles 60 ° and 130 ° and negative for the remaining stroke angles.

6.3 Comparison with theoretical and experimental results

For each of the case, non-dimensional displacement per cycle time is measured and compared with the results of slender-body theory (SBT) and resistive-force theory (RFT). Fig. 5 illustrates the effect of hydrodynamic interaction on the net displacement of swimmer with different stroke angles. The displacement per cycle as a function of stroke angle obtained from RFT is illustrated by solid line with square symbol, while the dashed lines with rhombus symbol are the results from SBT. The dotted lines with triangle symbol are the simulations results obtained in this study. Brian′s swimmer experiment, which was conducted only for one stroke angle, is given by an X symbol.

All these results indicate that the displacement direction is reversed for the stroke angles from 220 ° to 240 °. The results obtained from our simulations and from theories are still qualitatively consistent—the direction of motion and zero displacement stroke angles are the same, just the magnitude of the displacement differ slightly from each other.

6.4 Influence of flapping frequency in hydrodynamic force

CFD methodology offers convenient ways to alter any parameter involved in the study. We have continued simulation for various flapping frequency and found that the frequency also plays an important role in determining the hydrodynamic force and direction of swimming.

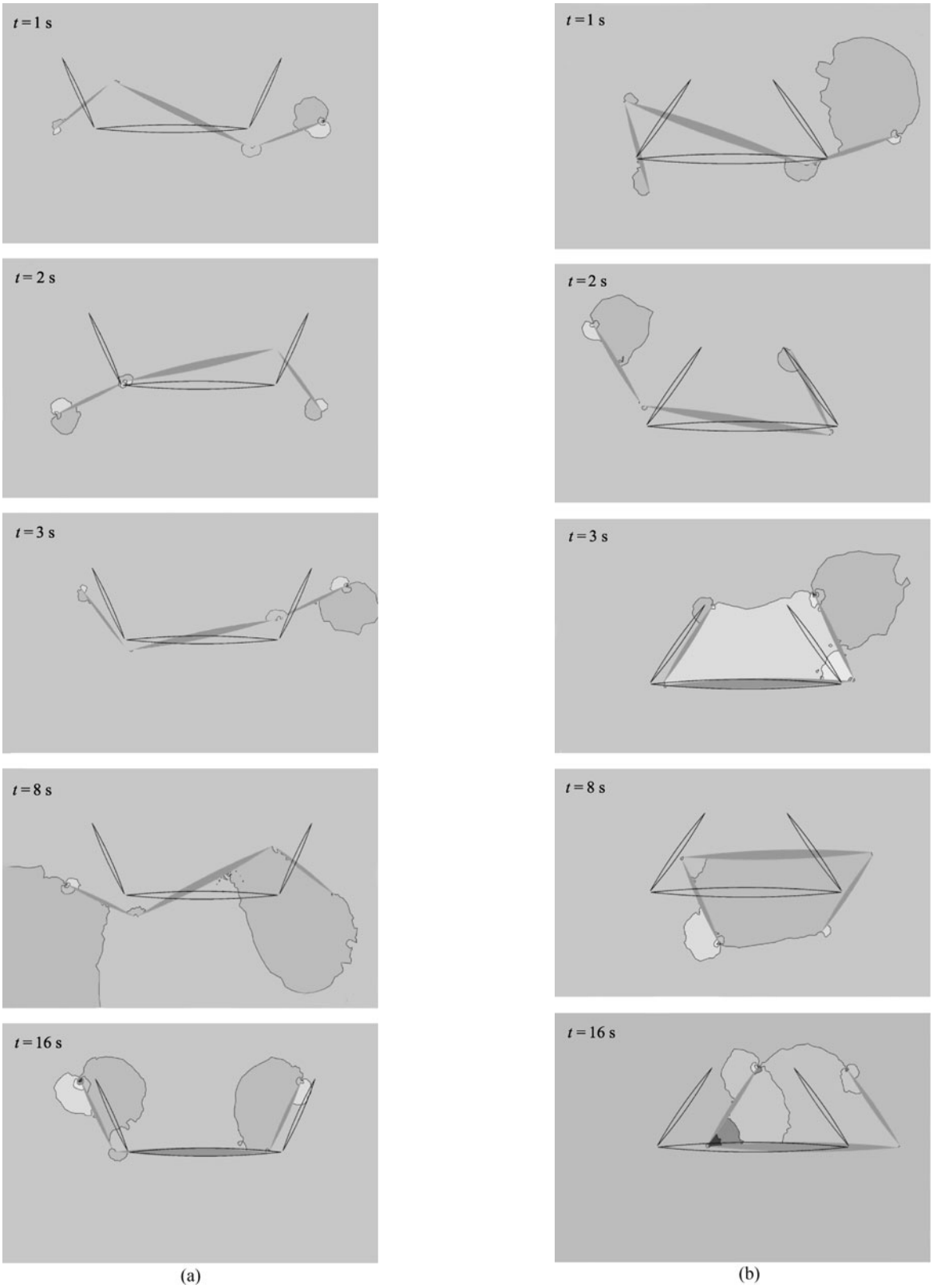

Fig. 3 (a) Pressure contours during swimming motion with stroke angle 130° at times 1 s, 2 s, 3 s, 8 s and 16 s. The net horizontal displacement is in forward direction after four cycle time (16 s); (b) Pressure contours at different time intervals when stroke angle is 250°, the net horizontal displacement after four cycles time is backward. See the attached movies for complete details

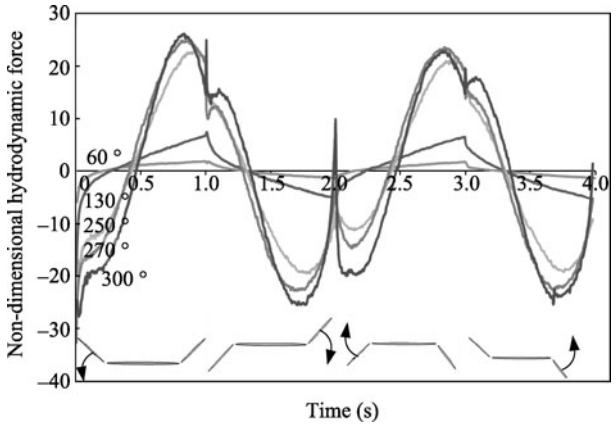

Fig. 4 Non-dimensional hydrodynamic force in the horizontal direction during the swimming motion for various stroke angles. The corresponding configurations of the links for each interval are at the bottom

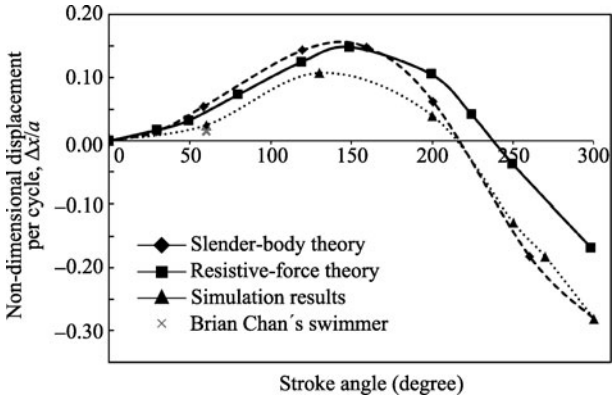

Fig. 5 The effect of stroke angle in non-dimensional horizontal displacement. A comparison of theories, experiment and our simulation show consistent results

Although the governing Stoke equations (1) and (2) are linear and time independent, the hydrodynamic force generated shows dependency on frequency at least in low frequency range as in Fig. 6. The magnitude of hydrodynamic force is nearly directly proportional to the frequency in low frequency domain (till 0.5 Hz). At frequency above 0.5 Hz, the magnitude of hydrodynamic force is becoming constant. This should be due to the fact that at low frequency, the boundary condition of the surfaces is in contact with the fluid for more time and hence making the flow as time-dependent Stoke flow.

Fig. 6 also shows the details of direction of the hydrodynamic force. For angles like 60 ° and 130 °, lower frequency causes backward swimming motion and higher frequency produces forward motion. For angles like 250 ° and 300 °, low frequency causes forward motion and high frequency backward motion. More importantly it is found that irrespective of the stroke angle, for the frequency range 0.30 to 0.35 Hz no mean hydrodynamic force is generated. This situation is similar to zero-displacement stroke angles (220 ° to 240 °) where there is no net translation. According to (1) and (2), the motion should be independent of frequency, but our simulation shows frequency dependence. Therefore this leads to the breakdown of Stokes law with inertia.

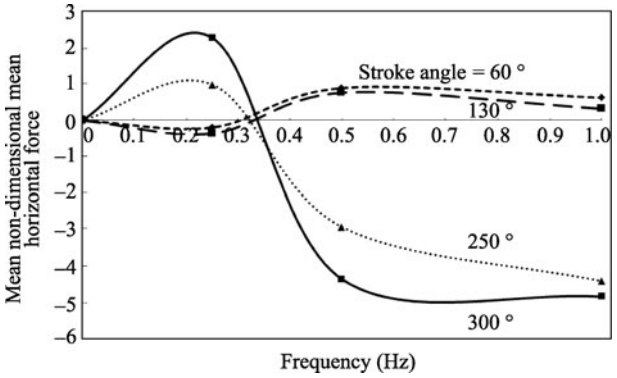

Fig. 6 Influence of flapping frequency on swimming direction for stroke angles 60 ° to 300 °. No net hydrodynamic force is generated for the frequency range 0.30–0.35 Hz

7 Conclusions and future work

In the present study, geometry and mesh of a Purcell′s three-linked swimmer is constructed, and the hydrodynamic interaction of the swimmer with the fluid is computed using CFD techniques. We visualized the pressure distribution around the links of the swimmer and computed mean hydrodynamic force acting on swimmer along the horizontal direction. We showed that changing stroke angle affects the force generated during swimming motion. These results are in accordance with the existing theories on very low Reynolds number flow and experimental observation by Brian. So far it has been thought, only stroke angle can change the direction of swimming but we have showed that even flapping frequency can change swimmer′s direction. All of these results are helpful in understanding the complex fluid mechanics behind the three-linked swimmer and deciding the parameters of swimmer for effective swimming.

There are many reported studies to realize the bacterial motion in micro- and nano-scale[15, 16] optimizing them using similar CFD methodology will help us in designing efficient and powerful swimming robots for specific applications.

For future work, we planned to investigate the case of flexible swimmer and considering the dimensions of the links. Extending to three dimensional simulation may also provide the most accurate and realistic numerical simulation of flapping motion of the swimmer.

References

[1] S. Childress. *Mechanics of Swimming and Flying*, Cambridge, UK: Cambridge University Press, 1977.

[2] E. M. Purcell. Life at low Reynolds number. *American Journal of Physics*, vol. 45, no. 1, pp. 3–11, 1977.

[3] R. Gilad, A. Porat, S. Trachtenberg. Motility modes of Spiroplasma melliferum BC3: A helical, wall-less bacterium driven by linear motor. *Molecular Microbiology*, vol. 47, no. 3, pp. 657–669, 2003.

[4] L. Becker, S. A. Koehler, H. A. Stone. Purcell′s swimmer: Which way does it go? In *Proceedings of the 53rd Annual*

Meeting of the Division of Fluid Dynamics, Washington, USA, 2000.

[5] L. E. Becker, S. A. Koehler, H. A. Stone. On self-propulsion of micro-machines at low Reynolds number: Purcell′s three-link swimmer. *Journal of Fluid Mechanics*, vol. 490, pp. 15–35, 2003.

[6] A. Naja, R. Golestanian. Simple swimmer at low Reynolds number: Three linked spheres. *Physical Review E*, vol. 69, no. 6, 062901, 2004.

[7] J. E. Avron, O. Raz. A geometric theory of swimming: Purcell′s swimmer and its symmetrized cousin. *New Journal of Physics*, vol. 10, 063016, 2008.

[8] M. S. Kumar, P. Philominathan. The physics of flagellar motion of *E. coli* during chemotaxis. *Biophysical Reviews*, vol. 2, no. 1, pp. 13–20, 2010.

[9] J. Gray, G. Hancock. The propulsion of sea-urchin spermatozoa. *Journal of Experimental Biology*, vol. 32, no. 4, pp. 802–814, 1955.

[10] J. Keller, S. Rubinow. Slender-body theory for slow viscous flow. *Journal of Fluid Mechanics*, vol. 75, no. 4, pp. 705–714, 1976.

[11] M. Bzdega, B. D. Robertson, R. Soller, G. Huber, S. A. Koehler. Motion of a robotic Purcell-type swimmer in a granular medium, to be published.

[12] C. Brian. Bio-inspired Fluid Locomotion, Ph. D. dissertation, Mechanical Engineering, Massachusetts Institute of Technology, USA, 2009.

[13] M. Kim, J. C. Bird, A. J. V. Parys, K. S. Breuer, T. R. Powers. A macroscopic scale model of bacterial flagellar bundling. *Proceedings of the National Academy of Sciences of the United States of America*, vol. 100, no. 26, pp. 15481–15485, 2003.

[14] ANSYS® Fluent, Flows using sliding and dynamic meshes, *Help System*, ANSYS, Inc., 2010.

[15] X. F. Ye, B. F. Gao, S. X. Guo, L. Q. Wang. Development of ICPF actuated underwater microrobots. *International Journal of Automation and Computing*, vol. 3, no. 4, pp. 382–391, 2006.

[16] W. Zhang, S. X. Guo, K. Asaka. A new type of hybrid fish-like microrobot. *International Journal of Automation and Computing*, vol. 3, no. 4, pp. 358–365, 2006.

M. Siva Kumar received his B. Sc. and M. Sc. degrees in physics from Bharathidasan University, India in 1993 and 1995, respectively, and the M. Ed. degree from Annamalai University, India in 1997. He was heading the Department of Physics in Indian School Muscat and now teaching in Oman Dental College. He has published several papers on bacterial motion and submitted his doctoral thesis on very low Reynolds number bacterial swimming motion.

His research interests include flagellar hydrodynamics and computational fluid dynamics.

E-mail: shiva@eeclubs.org

P. Philominathan graduated from St. Joseph′s College, Tiruchirappalli, Tamilnadu, India and got his post-graduation from the same college and obtained his M. Phil. degree from AVVM Sri Pushpam College, Poondi. He got his Ph. D. degree from Bharathidasan University, Tiruchirappalli, Tamilnadu, India in 2001. Since then, his interest has been in the fields of nonlinear dynamics and on certain novel materials (in both bulk and thin-film form). He is currently the head of the Department of Research and Post Graduate Department of Physics, AVVM Sri Pushpam College (Autonomous), affiliated to Bharathidasan University, Tirchirappalli, Tamilnadu, India.

His research interests include nonlinear systems, potentially significant materials, and automation.

E-mail: philominathan@gmail.com (Corresponding author)